

# Double-Spirals Offer the Development of Preprogrammable Modular Metastructures

Mohsen Jafarpour,\* Stanislav N. Gorb, and Hamed Rajabi

**Metamaterials with adjustable, sometimes unusual properties offer advantages over conventional materials with predefined mechanical properties in many technological applications. A group of metamaterials, called modular metamaterials or metastructures, are developed through the arrangement of multiple, mostly similar building blocks. These modular structures can be assembled using prefabricated modules and reconfigured to promote efficiency and functionality. Herein, a novel modular metastructure is developed by taking advantage of the high compliance of preprogrammable double-spirals. First, the mechanical behavior of a four-module metastructure under tension, compression, rotation, and sliding is simulated using the finite-element method. Then, 3D printing and mechanical testing are used to illustrate the tunable anisotropic and asymmetric behavior of the spiral-based metastructures in practice. The results show the simple reconfiguration of the presented metastructure toward the desired functions. The mechanical behavior of single double-spirals and the characteristics that can be achieved through their combinations make our modular metastructure suitable for various applications in robotics, aerospace, and medical engineering.**

## 1. Introduction

Structured materials with unprecedented tunable properties have been increasingly developed in recent years and have found

M. Jafarpour, S. N. Gorb  
Functional Morphology and Biomechanics  
Institute of Zoology  
Kiel University  
Kiel 24118, Germany  
E-mail: mjafarpour@zoologie.uni-kiel.de

H. Rajabi  
Division of Mechanical Engineering and Design  
School of Engineering  
London South Bank University  
London SE1 0AA, UK

H. Rajabi  
Mechanical Intelligence Research Group  
South Bank Applied BioEngineering Research (SABER)  
School of Engineering  
London South Bank University  
London SE1 0AA, UK

 The ORCID identification number(s) for the author(s) of this article can be found under <https://doi.org/10.1002/adem.202300102>.

© 2023 The Authors. Advanced Engineering Materials published by Wiley-VCH GmbH. This is an open access article under the terms of the Creative Commons Attribution License, which permits use, distribution and reproduction in any medium, provided the original work is properly cited.

DOI: [10.1002/adem.202300102](https://doi.org/10.1002/adem.202300102)

applications in robotics,<sup>[1,2]</sup> electronics,<sup>[3]</sup> energy harvesting systems,<sup>[4,5]</sup> biomedical engineering,<sup>[6]</sup> aerospace engineering,<sup>[7,8]</sup> structural engineering,<sup>[9]</sup> etc.<sup>[10–12]</sup> These materials, which are referred to as metamaterials, are engineered to exhibit properties that are derived from their architecture, rather than constituent materials.<sup>[13,14]</sup> Negative swelling ratio,<sup>[10]</sup> negative thermal expansion coefficient,<sup>[15]</sup> negative Poisson's ratio,<sup>[16]</sup> negative moduli,<sup>[17]</sup> anisotropic behavior,<sup>[18,19]</sup> reversible nonlinear deformability,<sup>[20,21]</sup> programmability,<sup>[22,23]</sup> and shape memorability<sup>[24]</sup> are some of the obtained mechanical properties.

Modular metamaterials consist of rationally designed modules or unit cells linked to each other. In these materials, desired mechanical properties can be achieved by engineered deformation of the consisting modules.<sup>[25–27]</sup> Hence, knowing the characteristics of each module is crucial when developing a metamaterial.

The geometry, material composition, and spatial arrangement of modules are key factors that determine the behavior of modular metamaterials under different boundary conditions and loadings. Structures used as modules for the development of modular metamaterials vary from rotating rigid shapes,<sup>[28–31]</sup> the wide range of honeycomb designs,<sup>[32–34]</sup> and re-entrant structures<sup>[35–37]</sup> to horseshoe-shaped structures,<sup>[10]</sup> foldable obelisk-like units,<sup>[25]</sup> bioinspired double-layer hinges,<sup>[38]</sup> helical structures,<sup>[39]</sup> and many other different designs.<sup>[2,19,22,40,41]</sup>

The aim of this study is to investigate the potential of preprogrammable compliant double-spiral structures, which have been recently introduced by our team, when used as the modules of a metastructure. Adjustable design, multiple degrees of freedom, high extensibility, and reversible nonlinear deformability are properties of the double-spirals that make them particularly interesting for the development of deformable structures.<sup>[42]</sup> We expect that preprogrammable double-spiral modules will enable us to control the mechanical properties of a metastructure in different directions in a passive-automatic way.

Using the finite-element method (FEM), we simulate the mechanical behavior of a four-module metastructure under different loading scenarios. We also manufacture two modular metastructures using 3D printing and illustrate their performance in practice. Our results show that the combination of different double-spirals can lead to tunable anisotropy, asymmetric behavior, preprogrammable shape change, spatial heterogeneity, and simple reconfiguration of the developed metastructure.

## 2. Experimental Section

### 2.1. Modeling and Finite-Element Analysis

Following the method adopted by Jafarpour et al.,<sup>[42]</sup> we used the equation of logarithmic spirals in the polar coordinate system (Equation (1)) to plot spiral curves using the programming software MATLAB (MathWorks).

$$r = r_0 e^{-k\theta} \quad (1)$$

In the above equation,  $r_0$  is the radius of the spiral at  $\theta = 0$ , and  $k$  is the polar slope.<sup>[43]</sup>

We plotted two logarithmic spirals with different initial radii ( $r_{0,1} = 13.5$  mm and  $r_{0,2} = 15.0$  mm) but an equal polar slope ( $k = 0.2$ ) from 0 to  $1.5\pi$  radians. We then rotated them around the origin of the coordinate system by  $\pi$  radian to generate two other spirals. These four spiral curves formed two spiral surfaces (Figure 1a). After connecting the bases and the ends of spirals with straight lines, the plot was imported to the finite-element software package ABAQUS/Standard v. 6.14 (SIMULIA) to

develop the 2D numerical model of the first double-spiral, named double-spiral 1 (Figure 1b).

The same procedure was used to develop a geometrically different double-spiral to investigate the behavior of a combination of double-spirals employed as the modules of a modular metastructure. We set the initial thickness, polar slope, and angle of rotation of double-spiral 2 to be 3 mm ( $r_{0,2} - r_{0,1} = 15 - 12 = 3.0$  mm), 0.1, and  $3\pi$  radians, respectively (Figure 1b). The values of the design variables were selected to obtain models with significantly different geometries. Double-spiral 1 is much shorter, thinner, and more curved than to double-spiral 2.

A modular metastructure, in which double-spiral modules were connected to blocks forming a square, was designed here (Figure 1c). We employed two models of each double-spiral 1 and 2 to develop a four-module metastructure (Figure 1d). We used this planar model to simulate its mechanical behavior subjected to in-plane loading scenarios in Abaqus. The model was meshed using four-node bilinear plane-stress quadrilateral elements with reduced integration (CPS4R). A mesh sensitivity analysis was conducted to set the size of the elements. The 0.1 mm elements resulted in accurate solutions in reasonable computational time.

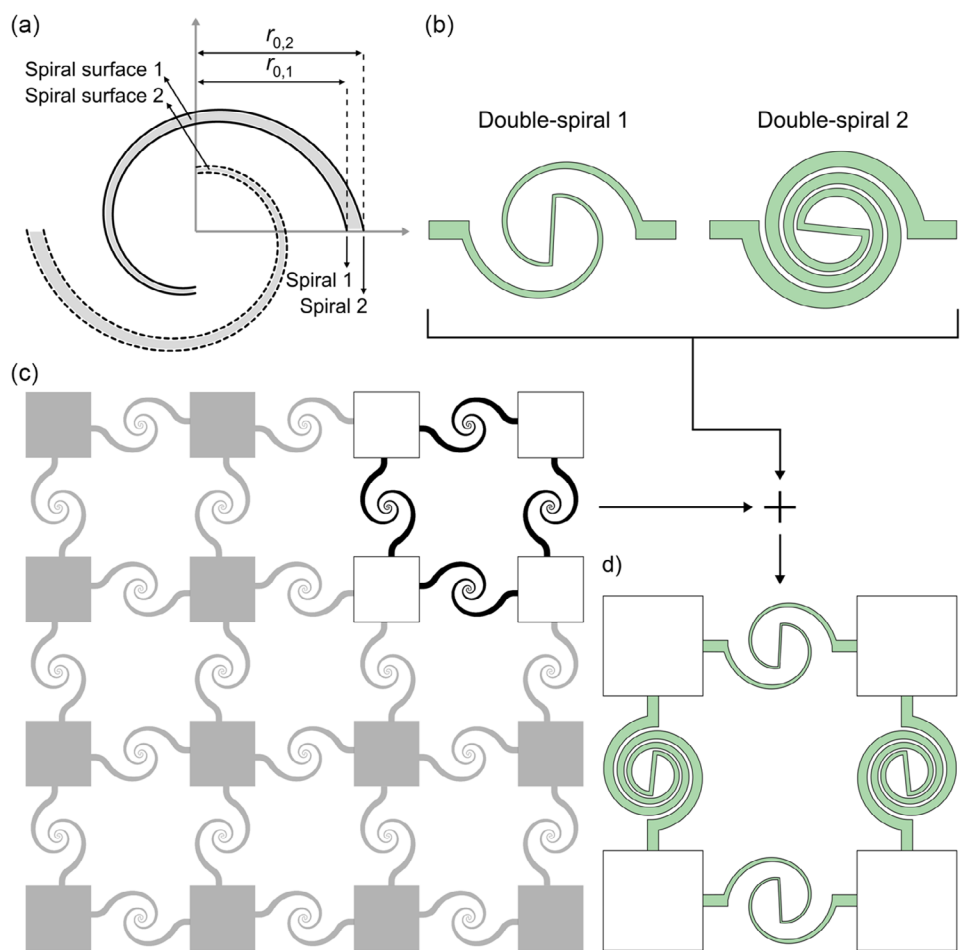


**Figure 1.** Development of the 2D models of double-spirals and four-module metastructure. a) Plotting four spiral curves to generate two spiral surfaces for the development of double-spiral 1. b) Double-spiral 1 and 2 models. c) A modular metastructure consisting of double-spiral modules connected to blocks. d) Using double-spirals 1 and 2 to develop a four-module metastructure.

**Table 1.** Mechanical properties of the thermoplastic polyurethane filament (Flexfill TPU 98A, Filamentum addi(c)itive polymers, Czech Republic).<sup>[45]</sup>

Density [kg m <sup>-3</sup> ]	Strain
1230	
Poisson's ratio	
0.3	
Stress [MPa]	Strain
0	0
12.1	0.1
22.1	0.5
28.4	1.0
37.8	3.0

We used the self-contact formulation in Abaqus to define the physical contacts between interacting surfaces.<sup>[44]</sup>

The material properties of the thermoplastic polyurethane (Flexfill TPU 98A, Filamentum addi(c)itive polymers, Czech Republic) presented in **Table 1** were assigned to the model.<sup>[45]</sup>

We used the Abaqus implicit solver to simulate the quasistatic behavior of the model under different loading scenarios. In all loading scenarios, the boundary conditions and loads were applied to the rigid blocks that were connected to the double-spirals. We avoided the large strain behavior of the elements and focused on reversible elastic deformations by limiting the load values. The following loading scenarios were simulated to characterize the performance of the spiral-based modular metastructure (**Figure 2**).

### 2.1.1. Tension

In this loading scenario, we extended the model once in the vertical and once in the horizontal directions (with respect to the horizon). In both cases, we clamped the model on one side and pulled it on the opposite side until the double-spirals reached their maximum lengths (**Figure 2a**).

### 2.1.2. Compression

Here we compressed the model twice in two perpendicular directions, while the blocks on the opposite side were fixed (**Figure 2b**). The compression was accomplished by applying a 2 N force.

### 2.1.3. Rotation

Under rotation, the model was clamped at the two opposite blocks b1 and b3, and then only one of the two other blocks, that is, b2, was subjected to a counterclockwise (CCW) moment (equal to 50 N.mm). Under the same loading and boundary condition, we then rotated the same block clockwise (CW) (**Figure 2c**).

### 2.1.4. Sliding

In this loading scenario, first, we fixed the blocks on one side, here b1 and b4, and pulled one of the two other blocks, that is, b3, downward by 50 mm, whereas b2 could move only vertically. We then clamped the model at a different side, that is, b3 and b4, and pulled b2 horizontally to reach the same displacement, while b1 was restricted in the vertical direction (**Figure 2d**).

## 2.2. Prototyping and Mechanical Testing

We manufactured two double-spirals from the numerical simulations with a fused deposition modeling (FDM) 3D printer (Prusa i3 MK3S, Prusa Research, Praha, Czech Republic) to test their behavior and validate the results of the simulations. Double-spirals and fixtures were printed using a semiflexible polyurethane filament (Flexfill TPU 98A, Filamentum addi(c)itive polymers, Czech Republic) and a polylactic acid (PLA) filament (Prusa Research, Praha, Czech Republic), respectively. A ZwickiLine uniaxial testing machine (Zwick Roell, Ulm, Germany) equipped with a 500 N load cell (Xforce P load cell, Zwick Roell) was used to quantify the tensile behavior of the manufactured double-spirals. Three specimens of each double-spiral were tested (three times each) under the same loading and boundary conditions used in the numerical simulations of the tension (**Figure 3**).

In the next step, we fabricated three double-spirals with distinct geometries using TPU filament and connected them to each other using connecting blocks made of PLA to develop modular metastructures with adjustable properties. We then tested their mechanical performance in practice. The values selected for design variables to obtain the 3D models of double-spirals, and the 3D printing settings are given in **Table 2**. We assembled the printed parts to make a beam-like and a cubic metastructure and characterized their behavior in two different experiments. First, we fixed one end of the beam structure and applied a 250-N.mm moment to its other end to investigate its behavior in bending (**Figure 4**). Then we used our uniaxial testing machine to quantify the compressive behavior of the cubic structure in three different directions (**Figure 5**).

## 3. Results

### 3.1. Finite-Element Analysis

The double-spirals, their arrangement in the presented metastructures, and used loading scenarios are only a few examples of the many potential combinations of design, loading, and boundary conditions. We presented these specific combinations to illustrate the potentials of our modular metastructure for a range of practical applications.

The force–displacement diagram that resulted from the simulation of tension showed that both tensile force and displacement in the vertical direction were about twice those in the horizontal direction (**Figure 2a**). The force–displacement diagram corresponding to the compression showed that the metastructure was about six times more compliant under compression in the horizontal direction than in the vertical direction (**Figure 2b**). These two loadings show the anisotropy of the developed metastructure.

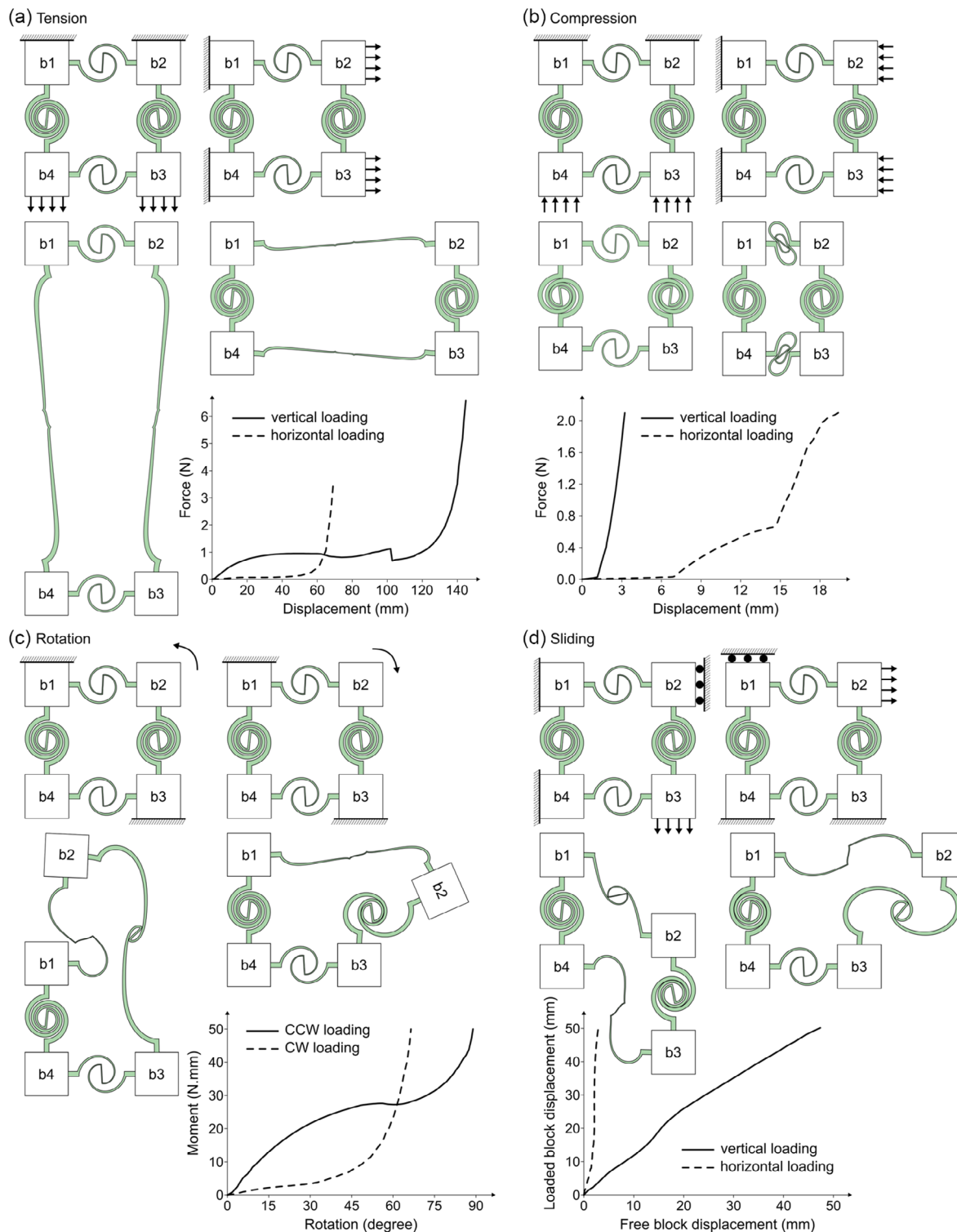


**Figure 2.** Simulation of the mechanical behavior of the four-module metastructure model. Results are given for the following loading scenarios: in-plane a) tension, b) compression, c) rotation, and d) sliding. Shaded areas show the fixed boundary conditions, and arrows show the direction of applied loads.

Rotating a block of the model (b2 in Figure 2c) in two opposite directions (CW and CCW) demonstrated its asymmetric behavior. Although the rotational deflections of b2 subjected to the

same moment in two directions were not much different, the work required for the CCW deformation was about four times that for the CW deformation. The moment-rotation diagram

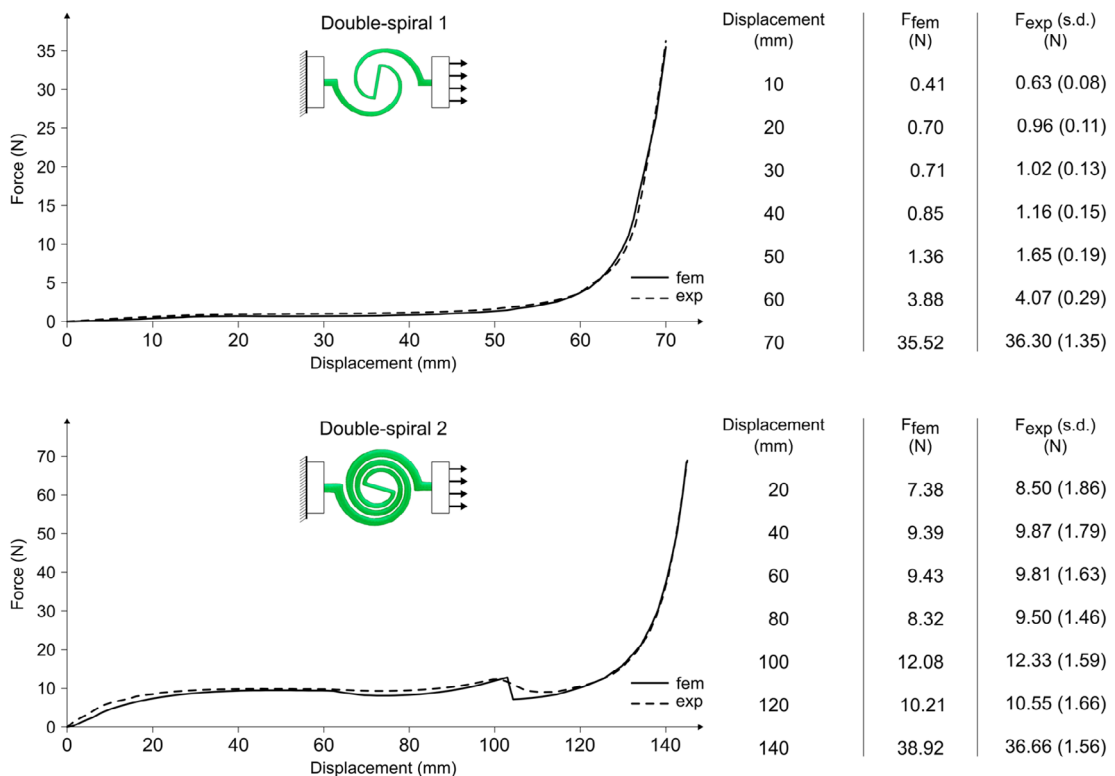


**Figure 3.** 3D printing and testing of two double-spirals from the numerical simulations. Comparison of the force–displacement curves and force values obtained from the numerical and experimental tensile tests on double-spirals 1 and 2.

**Table 2.** Double-spiral models developed for 3D printing, besides their corresponding values of design variables, and settings used for 3D printing.

3D modeling				
Developed double-spirals	Double-spiral 1	Double-spiral 2	Double-spiral 3	
Design variables	Polar slope Initial thickness [mm] Angle of rotation [rad] Extrusion height [mm]	0.10 3.0 $3\pi$ 20	0.20 2.5 $1.5\pi$ 20	0.05 1.0 $4\pi$ 20
3D printing settings				
Filament type	Thermoplastic polyurethane		Polylactic acid	
Filament name	Flexfill TPU 98A		PLA	
Produced by	Fillamentum addi(c)tive polymers, Czech Republic		Prusa Research, Praha, Czech Republic	
Filament diameter [mm]	1.75		1.75	
Nozzle diameter [mm]	0.4		0.4	
Extrusion temperature [°C]	240		215	
Bed temperature [°C]	50		60	
Layer height [mm]	0.2		0.2	
Fill pattern	Gyroid		Gyroid	
Fill density [%]	20		20	

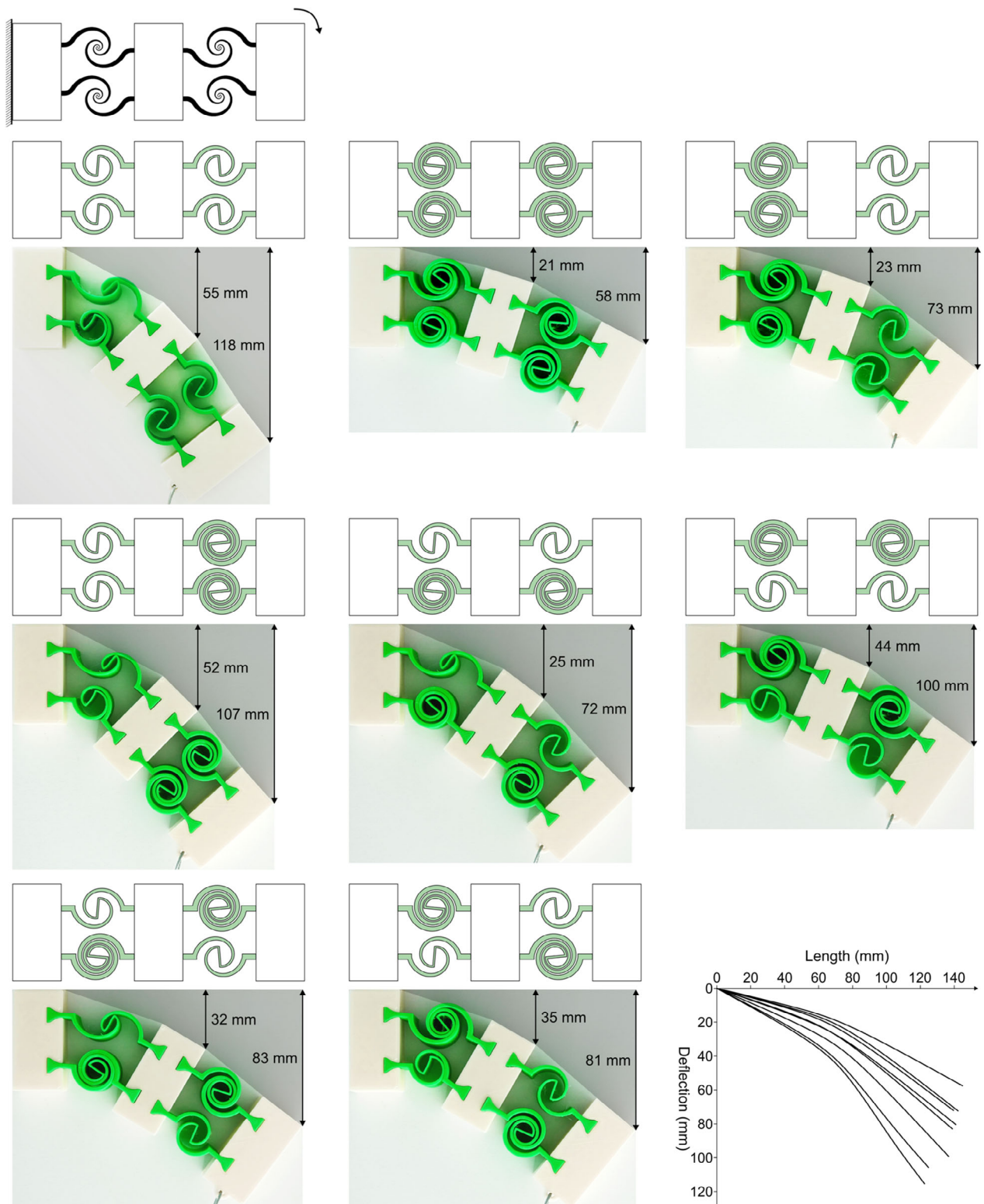


**Figure 4.** 3D printing and testing of a beam-like modular metastructure. Eight structures were developed using double-spirals 1 and 2 arranged in eight different ways. The structures were fixed at one end and a 250-N-mm moment was applied to their free end. Shaded area shows the fixed boundary condition, and the arrow shows the direction of the applied moment. The deflections of the loaded structures can be compared using the displacement values written next to the blocks and the diagrams illustrating their deflections all together.

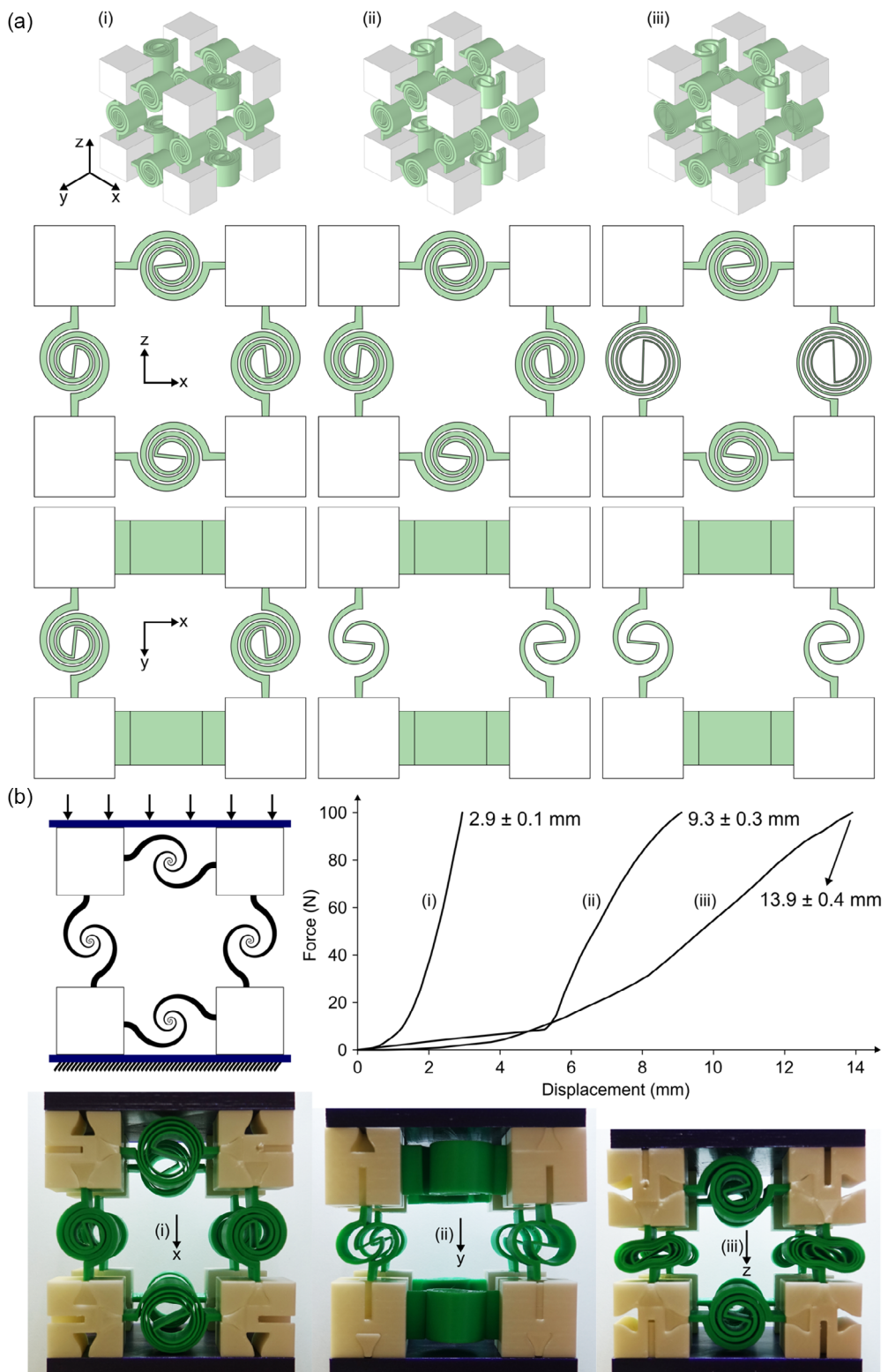


**Figure 5.** 3D printing and testing of a cubic modular metastructure. a) Three cubes were developed using double-spirals 1, 2, and 3. b) The third cube was placed between two plates, and a 100-N force was used to displace one plate toward the other one that was fixed. The force–displacement diagram shows the anisotropic behavior of the cubic metastructure in x, y, and z directions. The average values of the maximum displacement ( $n = 5$ ) and their standard deviations are written next to the corresponding curves.

shows the different stiffnesses of the metastructure in the two directions and their variations as the deformation increases (Figure 2c).

The force–displacement diagrams illustrate the nonlinear behavior of the metastructure, related to the specific phases of the deformation of double-spirals under different loading scenarios (i.e., initial clearance, unrolling, and unfolding).<sup>[42]</sup> The tension and rotation of the metastructure in two different directions occur with an inversion of anisotropy. In tension, 0.5-N force is enough to unroll double-spiral 1 horizontally and reach the high-stiffness unfolding phase (around 60-mm displacement). However, the vertical 0.5-N force extends double-spiral 2 by only 10 mm. Nevertheless, the metastructure has higher extensibility in the vertical direction when it is subjected to larger tensile forces. The same scenario lies behind the inversion of anisotropy in the CW and CCW rotations of the metastructure.

We used the sliding scenario to indicate the behavior of the free block which was not loaded (b2 in the vertical sliding and b1 in the horizontal sliding, Figure 2d). In the vertical loading, the displacement of the loaded block (b3) led to almost the same displacement of the free block (b2). However, in the horizontal loading, when we moved the block (b2) horizontally, the free block (b1) did not move and therefore the whole structure showed a different deformation pattern compared to the vertical loading (Figure 2d).

### 3.2. Prototyping and Mechanical Testing

Here, we 3D printed the double-spirals used in numerical simulations and characterized their tensile behavior experimentally to verify the validity of the simulations. To this goal, we averaged the force–displacement curves from the experiments ( $n=9$ ) and compared that to the numerical force–displacement curve (Figure 3). We measured the quality of the fit by comparing the average force values that resulted from the two methods at the same displacements. The comparisons show that for both double-spirals, a good agreement exists between the numerical and experimental J-shaped curves.

Two spiral-based metastructures were manufactured and tested in the next step. First, a beam-like modular metastructure was developed using double-spirals 1 and 2, that were horizontally connected to three blocks (Figure 4). Two geometrically different double-spirals were employed in eight arrangements. Fixing one end of these structures and applying an equal moment to their free end resulted in different deformation patterns. The deflection of the middle point of beams varied from 21 to 55 mm, and the deflection of their tip varied from 53 to 118 mm. This demonstrates the asymmetric behavior and tunable structural stiffness of the developed structures that results from the different combinations of two double-spirals with different thicknesses, lengths, and polar slopes.

We then used double-spirals 1, 2, and 3 to connect eight blocks in the form of a cube and developed three cubic modular metastructures (Figure 5a). The first cube was made up of double-spiral 1 only and was expected to have the same compressive stiffness in all three directions of the Cartesian coordinate system (Figure 5a-i). The second cube, consisting of double-spirals 1 and

2, could behave the same in  $x$  and  $z$  directions, but different in  $y$  direction (Figure 5a-ii).

To have a cubic metastructure with a specific mechanical characteristic in each direction, we used four of each double-spirals 1, 2, and 3 and developed the third cube (Figure 5a-iii). The compressive behavior of this cube was quantified in three directions (Figure 5b). We placed it between two plates and used a 100-N force to displace one plate toward the other one that was fixed. Repeating this test five times in each direction resulted in 2.9 ( $\pm 0.1$ ) mm, 9.3 ( $\pm 0.3$ ) mm, and 13.9 ( $\pm 0.4$ ) mm displacement of the plate in the  $x$ ,  $y$ , and  $z$  direction, respectively. The compression of the double-spirals starts with a low-stiffness deformation phase, which arises from the free space between their coils, and continues with a gradual increase in the stiffness, which results from the contact between the coils.<sup>[42]</sup> The different compressive behaviors of the metastructure in  $x$ ,  $y$ , and  $z$  directions are mainly caused by the different free space available between the coils of the double-spirals and their thicknesses, which can be simply adjusted by changing the values of the design variables.

## 4. Discussion

Modular metastructures consisting of exchangeable modules can be used in different applications in which simple adjustability is a requirement. In this study, we used only two/three geometrically different double-spirals as modules of spiral-based modular metastructures to obtain distinct mechanical behaviors under the same load. Our results showed that the geometrical design variables of the double-spirals can be used to preprogram the behaviors observed. The spatial arrangement of the double-spirals, type of loading, and boundary condition determine the behavior of the spiral-based modular metastructure.

Using our double-spirals in the developed metastructure enabled us to tune the stiffness of the metastructure in different directions and how it changes during the application of the external loads. Our results illustrated the high reversible extensibility, variable stiffness, anisotropy, and asymmetric behavior of the developed metastructures. We could tune all these features by changing the design variables of the double-spirals and controlling the structural stiffness in each direction. These characteristics can be a great advantage to many engineering structures, such as mechanical hinges<sup>[46,47]</sup> biomedical implants,<sup>[19]</sup> asymmetric casts and splints,<sup>[48]</sup> flexible body armors,<sup>[49]</sup> and load-bearing yet collision-resistant kites.<sup>[50]</sup>

Programmed shape change in response to mechanical loads is another interesting property of the metastructures. Shape changes can enable engineering structures to transform into predictable shapes when loaded, to change their performance and/or improve their efficiency.<sup>[22,23]</sup> In this study, the sliding loading scenario conducted horizontally and vertically resulted in two different deformation patterns (Figure 2d). The difference is due to the internal boundary condition that double-spirals passively apply on each block. Numerical and experimental results suggest that this shape change can be preprogrammed using different double-spirals with suitable geometrical design variables (Figure 2d, 4). Varying the orientation of the modules from the horizontal and vertical directions to angled directions is another strategy that can also change the local boundary

condition on the blocks and influence the behavior of the metastructure.

Since the modular metastructure developed here comprises individual modules, the dimensions of the metastructure can be easily changed by adding or removing double-spirals. Employing double-spirals with various mechanical behaviors in a larger structure could result in the spatial heterogeneity or gradient of properties. However, there is a constraint against increasing this heterogeneity. Complex aperiodic architectures could hinder the desired functionality of a structure and prevent its coherent and predictable response.<sup>[22,51]</sup> Therefore, any design should provide a trade-off between the high level of controllability and complexity.

In this study, we presented the concept of using compliant double-spirals as the modules of a modular metastructure. The results showed the potential of double-spirals for this purpose. Considering that our simulations were conducted on small assemblies of double-spirals, future studies should focus on characterizing the behavior of spiral-based metastructures in large scales. A combinatorial design theory,<sup>[22]</sup> an inverse-design method,<sup>[51]</sup> and a structural stiffness matrix-based computational method<sup>[52]</sup> are a few examples that can be used to predict the mechanical behavior of large spiral-based modular metastructures. Further investigations should examine the performance of the double-spirals with different geometries and material compositions under long-term loadings. Artificial intelligence (AI) has progressed researches on metamaterials significantly<sup>[12]</sup> and can be used in the future studies to obtain double-spirals with geometries optimized for specific applications. The arrangement of the modules in the developed metastructure is another factor that remains to be tested to improve its mechanical behavior.

## 5. Conclusion

In this article, we presented a modular metastructure that consists of compliant double-spirals and investigated its mechanical behavior under different loading scenarios. Our results showed that by combining double-spirals in specific configurations, we can exploit desired properties, including tunable anisotropy, asymmetric behavior, preprogrammable shape change, and spatial heterogeneity, besides the advantageous features of single double-spirals, such as simply adjustable design, multiple degrees of freedom, high extensibility, and reversible nonlinear deformability. Furthermore, if any unexpected modification is necessary, the use of independently exchangeable modules in the modular metastructure makes its reconfiguration feasible. Individual double-spirals could be printed fast at low costs using a single material and be readily assembled. The metastructure presented in this study can offer an alternative design for engineered materials that are currently in use in various engineering fields. Compact, yet highly extensible double-spirals make the metastructure adequate for aerospace engineering products which need to be portable and stowable. Highly tunable nonlinear deformations of the spiral-based metastructure in different directions suggest it could provide an efficient solution to the development of biomedical engineering devices for rehabilitation. The metastructure comprised preprogrammable

double-spirals, which control the motion of components in a passive-automatic way, could be of particular interest in articulated robots.

## Acknowledgements

The authors are grateful to Mr. Shahab Eshghi (Kiel University, Germany) for his helpful discussions.

Open Access funding enabled and organized by Projekt DEAL.

## Conflict of Interest

The authors declare no conflict of interest.

## Author Contributions

M.J. took care of conceptualization; data curation; formal analysis; funding acquisition; investigation; methodology; validation; visualization; writing the original draft; writing the review and editing; S.G. took care of conceptualization; funding acquisition; project administration; resources; supervision; writing the review and editing; H.R. took care of conceptualization; methodology; project administration; supervision; writing the review and editing.

## Data Availability Statement

The data that support the findings of this study are available from the corresponding author upon reasonable request.

## Keywords

3D printing, finite-element method, functional design, mechanical intelligence, structured materials

Received: January 23, 2023

Revised: March 8, 2023

Published online:

- [1] L. Wang, Y. Yang, Y. Chen, C. Majidi, F. Iida, E. Askounis, Q. Pei, *Mater. Today* **2018**, *21*, 563.
- [2] R. Khajehtourian, D. M. Kochmann, *Front. Rob. AI* **2021**, *8*, 121.
- [3] Y. Ma, X. Feng, J. A. Rogers, Y. Huang, Y. Zhang, *Lab Chip* **2017**, *17*, 1689.
- [4] P. Jiao, Y. Yang, K. I. Egbe, Z. He, Y. Lin, *ACS Omega* **2021**, *6*, 15348.
- [5] P. Jiao, H. Zhang, W. Li, *ACS Appl. Mater. Interfaces* **2023**, *15*, 2873.
- [6] K. I. Jang, H. U. Chung, S. Xu, C. H. Lee, H. Luan, J. Jeong, H. Cheng, G. T. Kim, S. Y. Han, J. W. Lee, J. Kim, *Nat. Commun.* **2015**, *6*, 6566.
- [7] G. Jefferson, T. A. Parthasarathy, R. J. Kerans, *Int. J. Solids Struct.* **2009**, *46*, 2372.
- [8] J. Morgan, S. P. Magleby, L. L. Howell, *J. Mech. Des.* **2016**, *138*, 052301.
- [9] L. Cveticanin, *Curr. Trends Civ. Struct. Eng.* **2020**, *6*, <https://doi.org/10.33552/ctcse.2020.06.000633>.
- [10] H. Zhang, X. Guo, J. Wu, D. Fang, Y. Zhang, *Sci. Adv.* **2018**, *4*, eaar8535.
- [11] J. U. Surjadi, L. Gao, H. Du, X. Li, X. Xiong, N. X. Fang, Y. Lu, *Adv. Eng. Mater.* **2019**, *21*, 1800864.
- [12] P. Jiao, A. H. Alavi, *Int. Mater. Rev.* **2021**, *66*, 365.

- [13] X. Yu, J. Zhou, H. Liang, Z. Jiang, L. Wu, *Prog. Mater. Sci.* **2018**, 94, 114.
- [14] K. Bertoldi, V. Vitelli, J. Christensen, M. Van Hecke, *Nat. Rev. Mater.* **2017**, 2, 17066.
- [15] J. Qu, M. Kadic, A. Naber, M. Wegener, *Sci. Rep.* **2017**, 7, 40643.
- [16] H. M. Kolken, A. A. Zadpoor, *RSC Adv.* **2017**, 7, 5111.
- [17] A. A. Zadpoor, *Mater. Horiz.* **2016**, 3, 371.
- [18] C. N. Layman, C. J. Naify, T. P. Martin, D. C. Calvo, G. J. Orris, *Phys. Rev. Lett.* **2013**, 111, 024302.
- [19] S. Xu, J. Shen, S. Zhou, X. Huang, Y. M. Xie, *Mater. Des.* **2016**, 93, 443.
- [20] D. Mousanezhad, H. Ebrahimi, B. Haghpanah, R. Ghosh, A. Ajdari, A. M. S. Hamouda, A. Vaziri, *Int. J. Solids Struct.* **2015**, 66, 218.
- [21] C. Bonatti, D. Mohr, *Int. J. Plast.* **2017**, 92, 122.
- [22] C. Coulais, E. Teomy, K. De Reus, Y. Shokef, M. Van Hecke, *Nature* **2016**, 535, 529.
- [23] M. Konaković-Luković, J. Panetta, K. Crane, M. Pauly, *ACM Trans. Graphics* **2018**, 37, 857.
- [24] J. Wang, L. Hong, P. Jiao, *Mater. Des.* **2023**, 226, 111648.
- [25] N. Yang, M. Zhang, R. Zhu, X. D. Niu, *Sci. Rep.* **2019**, 9, 18812.
- [26] W. Liu, H. Jiang, Y. Chen, *Adv. Funct. Mater.* **2022**, 32, 2109865.
- [27] J. J. Mao, S. Wang, W. Tan, M. Liu, *Eng. Struct.* **2022**, 272, 114976.
- [28] J. N. Grima, A. Alderson, K. E. Evans, *Phys. Status Solidi B* **2005**, 242, 561.
- [29] D. Attard, J. N. Grima, *Phys. Status Solidi B* **2008**, 245, 2395.
- [30] R. Gatt, L. Mizzi, J. I. Azzopardi, K. M. Azzopardi, D. Attard, A. Casha, J. Briffa, J. N. Grima, *Sci. Rep.* **2015**, 5, 8395.
- [31] A. Jamalimehr, M. Mirzajanzadeh, A. Akbarzadeh, D. Pasini, *Nat. Commun.* **2022**, 13, 1816.
- [32] D. Mousanezhad, B. Haghpanah, R. Ghosh, A. M. Hamouda, H. Nayeb-Hashemi, A. Vaziri, *Theor. Appl. Mech. Lett.* **2016**, 6, 81.
- [33] M. Bodaghi, A. R. Damanpack, G. F. Hu, W. H. Liao, *Mater. Des.* **2017**, 131, 81.
- [34] Y. Zhang, X. Ren, W. Jiang, D. Han, X. Y. Zhang, Y. Pan, Y. M. Xie, *Mater. Des.* **2022**, 221, 110956.
- [35] J. N. Grima, R. Gatt, A. Alderson, K. E. Evans, *Mol. Simul.* **2005**, 31, 925.
- [36] N. Xu, H. T. Liu, *Compos. Commun.* **2020**, 22, 100431.
- [37] X. Gong, C. Ren, J. Sun, P. Zhang, L. Du, F. Xie, *Biomimetics* **2022**, 7, 198.
- [38] H. Rajabi, S. H. Eragli, A. Khaheshi, A. Toofani, C. Hunt, R. J. Wootten, *Proc. Natl. Acad. Sci.* **2022**, 119, e2211861119.
- [39] G. Cimolai, I. Dayyani, Q. Qin, *Mater. Des.* **2022**, 215, 110444.
- [40] Z. Ma, J. Lin, X. Xu, Z. Ma, L. Tang, C. Sun, D. Li, C. Liu, Y. Zhong, L. Wang, *Int. J. Lightweight Mater. Manuf.* **2019**, 2, 57.
- [41] L. Dong, D. Wang, J. Wang, C. Jiang, H. Wang, B. Zhang, M. S. Wu, G. Gu, *Phys. Rev. Appl.* **2022**, 17, 044032.
- [42] M. Jafarpour, S. Gorb, H. Rajabi, *J. R. Soc. Interface* **2023**, 20, 20220757.
- [43] K. Tsuji, S. C. Müller, *Spirals and Vortices: In Culture, Nature, and Science*, Springer, Cham, Switzerland **2019**, p. 296.
- [44] M. Smith, *Abaqus/Standard User's Manual, Version 6.9*, Dassault Systèmes Simulia Corp, Providence, RI **2009**.
- [45] Fillamentum, and Addi(c)itive Polymers **2019** [Flexfill TPU 98A Technical Data Sheet].
- [46] J. Pinski, B. Shirinzadeh, M. Ghafarian, T. K. Das, A. Al-Jodah, R. Nowell, *Mech. Mach. Theory* **2020**, 150, 103874.
- [47] S. H. Eragli, A. Toofani, A. Khaheshi, M. Khorsandi, A. Darvizeh, S. Gorb, H. Rajabi, *Adv. Sci.* **2021**, 8, 2004383.
- [48] A. Khaheshi, S. N. Gorb, H. Rajabi, *Appl. Phys. A* **2021**, 127, 181.
- [49] P. Rawat, D. Zhu, M. Z. Rahman, F. Barthelat, *Acta Biomater.* **2021**, 121, 41.
- [50] A. Khaheshi, H. T. Tramsen, S. N. Gorb, H. Rajabi, *Mater. Des.* **2021**, 198, 109354.
- [51] N. Yang, J. L. Silverberg, *Proc. Natl. Acad. Sci.* **2017**, 114, 3590.
- [52] X. Yin, B. C. Wang, L. Liu, L. Y. Zhang, G. K. Xu, *J. Mech. Phys. Solids* **2022**, 169, 105077.